THE RESPONSE OF A 300μ SILICON DETECTOR TO MONOENERGETIC NEUTRONS DETERMINED BY THE USE OF THE MONTE CARLO TECHNICUE

M. Taherzadeh and G. Anno*

The Jet Propulsion Laboratory

The response of a 300μ thick silicon detector to an incident monoenergetic neutron beam is evaluated by the Monte Carlo method for the cases of both a shielded and a bare detector.

The result of Monte Carlo calculation, using elastic, inelastic and absorption reactions indicates that the response of the silicon detector to neutrons is basically due to the elastic scattering. In addition, the gamma rays generated in the shield of the detector will result in a response which is 3 or 4 orders of magnitude smaller than response to incident photons. The response of a bare silicon detector is calculated for neutron energies up to 6 MeV and bias energies from 50 to 250 KeV. It is found that the maximum response for a 300μ thick silicon detector is less than 4×10^{-3} c/n within this selected neutron and bias energy range. When the pulse height defect is introduced in the calculation the results at low energy neutrons were reduced.

INTRODUCTION

Nuclear radiation from an RTG used as the prime source of energy for electrical power in space science missions, can severely affect the scientific instruments or detectors aboard the spacecraft. These nuclear particles consist mainly of neutrons and gamma rays.

The neutrons and photons are emitted radially from the plutonium fuel power source with a flux level which depends upon the impurities and the age of the fuel itself. The interference between these radiations and the detectors in the science package unit, can take place via nuclear reactions. Therefore, it is necessary to identify these radiations and their effects on the detectors by a thorough analysis and evaluation of the radiation environment of the fuel and the responses that they produce in the science-experiment detectors..

In this paper, the response of a 300μ silicon detector to neutrons emitted from a plutonium dioxide fuel power source is determined. Neutrons released from the source not only interact directly with the detectors but also when detectors are shielded against primary photons additional radiation is generated by inelastic scattering and the radiative capture of the source neutrons within the shield.

RESPONSE OF A BARE DETECTOR

The response function of a 300μ bare silicon detector to neutrons can be studied by a Monte Carlo Code[1] using the probability laws of interactions and energy and angular distributions. However, in the case of a bare and a very thin detector (300μ) and low energy neutrons, the pulse height can be estimated easily via kinematical equations. This, of course, does not mean that we will be able to calculate the exact response by such a simplified scheme. Nevertheless, if we estimate the response of a silicon detector for a worst case and show it is much below the response to the primary gamma rays from the source the importance of neutrons as far as additional shielding is concerned would be reduced. Since our main interest in this analysis is the response to neutrons emanated from a PuO_2 nuclear power source, we should examine the neutron source spectrum first.

In Figure 1, the neutron flux and the flux spectrum of a typical PuO_2 fuel power source is presented. The fuel is a 2KW multihundred watt power source and emits a total of 4.59×10^4 neutrons/gmPuO_2/sec. At 50 cm away from the center of the source and at zero angle with respect to the major axis of the fuel, the total flux is 5.43×10^3 neutrons/cm^2/sec. From this flux distribution we conclude that the average neutron energy is about 2 MeV and the maximum neutron energy can be as high as 10 MeV or more but with a very small neutron abundance.

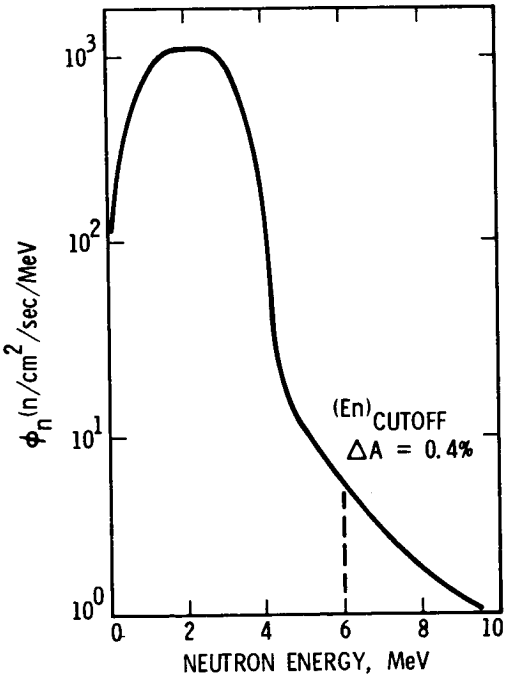

FIGURE 1. Neutron Flux Specrum of A 2KW PuO_2 Power Source (r = 50 cm and θ = 0.)

In order to limit ourselves with the number of nuclear reactions involved, we can arbitrarily set a maximum for the neutron energy so that the percent of the neutrons which will be ignored contributes an insignificant amount to the overall response of the detector. One such arbitrarily selected maximum energy is 6 MeV so that the neutrons with energies greater than 6 MeV contribution less than 0.5%.

Having selected a range of energies for the released neutrons, we can proceed to calculate the response of a silicon detector to a beam of neutrons emitted from a PuO_2 fuel power source. The total and the partial neutron cross sections as a function of neutron energies up to 6 MeV are presented in Figure 2. The reactions considered here are elastic scattering (n,n), inelastic scattering (n,n'γ), and the neutron disappearing reactions. These reactions consist of (n,α), (n,p) and the radiative capture reaction (n,γ).

The significant features of these cross sections are:

1. The (n,p) and the (n,α) reactions become important beyond a neutron energy of about 4.5 MeV, however, at these high neutron energies the neutron abundance diminishes very rapidly. For this reason reactions which are kinematically possible, but have high threshold energies such as (n,2n), are not included in this analysis, and the contribution from such reactions should be considered extremely small.

2. At low neutron energies (i.e., below 1.5 MeV), only two reactions are possible; they are elastic scattering and radiative capture.

3. In the medium range neutron energy, (i.e., between 1.5 to 5 MeV) the difference between the total cross section and the elastic scattering cross section increases with energy but never reaches 50% of the total cross section. This means, in this neutron energy range, the most important reaction is elastic scattering.

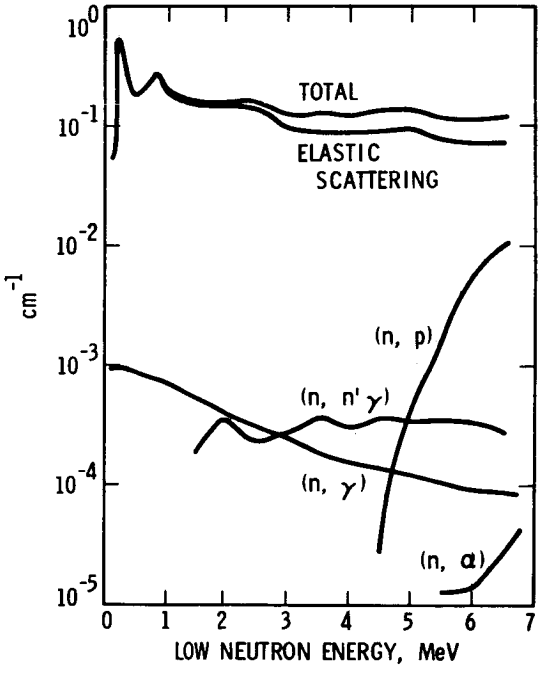

FIGURE 2. Neutron - Silicon Cross Section

Thus, the (n,p) and (n,α) reactions can be considered as a source of background while elastic scattering is by far the largest contributing reaction. The radiative capture (n,γ) and the inelastic scattering (n,n'γ) reactions have much smaller cross sections and the emitted photons escape the detector's sensitive area before depositing any energy. In Table 1, these neutron-silicon reactions are summarized with their corresponding threshold energies, Q-values, the emitted secondary particles, the neutron abundances at the threshold energies and the maximum energy and range of the outgoing particles in the silicon detector. The (n,2n) reaction is added to the list as an example of the reactions which will not be considered at all due to its high threshold energy and low neutron flux levels.

TABLE (1)
NEUTRON - SILICON REACTIONS
$(E_n)_{Max}$ = 6 MeV

	REACTIONS	$Si^{28}(n,b)R$	Q MeV	$(E_n)_{th}$ MeV	$(E_b)_{Max}$	ABUNDANCE at E_{th}	σ At 1.5 MJ barns
1)	NEUTRON DISAPPEARING	$Si^{28}(n,\alpha)Mg^{25}$	-2.7	2.66	2.68 (10μ)	13%	0
2)	NEUTRON DISAPPEARING	$(n,p)Al^{28}$	-3.9	3.66	1.81 (42μ)	8.3%	0
3)	ELASTIC SCATTERING	$(n,n)Si^{28}$	0.0	0.0	.798 (.45μ)	--	2.915
4)	INELASTIC SCATTERING	$(n,n'\gamma)Si^{28}$	0.0	0.0	--	--	3.64×10^{-3}
5)	RADIATIVE CAPTURE	$(n,\gamma)Si^{29}$	8.47	0.0	--	--	1.11×10^{-2}
6)	OTHER PARTICLE PRODUCING	$(n,2n)Si^{28}$	-8.47	8.81	--	.14%	0
7)	OTHER PARTICLE PRODUCING	$(n,np)Al^{27}$	-11.6	12.06	--	--	0

The response function of a detector medium at a given neutron energy and when pulse height defect is neglected is given by

$$R(E_n, E_B) = \epsilon_D(E_n)\, P(E_n, E_B) \qquad (1)$$

where E_B is the bias energy. The detector's efficiency function for normal incidence $\epsilon_D(E)$, is generally given by

$$\epsilon_D(E_n) = 1 - Exp\left[-\mu(E_n)t\right] \qquad (2)$$

$\mu(E)$ is the attenuation coefficient of the detector and t is the sensitive thickness. $P(E,E_B)$ is the probability that a transfer in energy to the silicon nucleus is above the bias energy E_B. The efficiency functions for (n,n), (n,p) and (n,α) reactions are presented in Figure 3 together with the total values for a 300μ silicon detector. The shape of these curves follows the total cross section because the effective thickness of the detector is small and

$$\epsilon_D(E_n) = N_D t\, \sigma(E_n) \qquad (3)$$

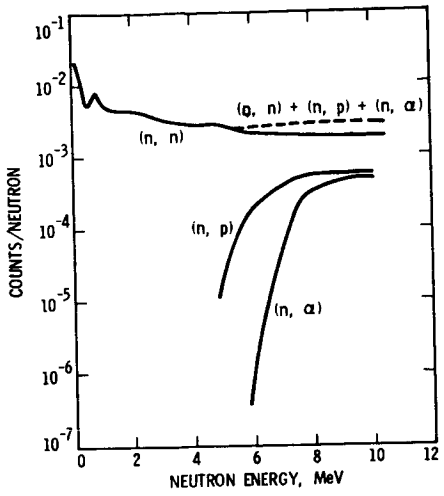

FIGURE 3. Zero Bias Efficiency of A 300μ Silicon Detector

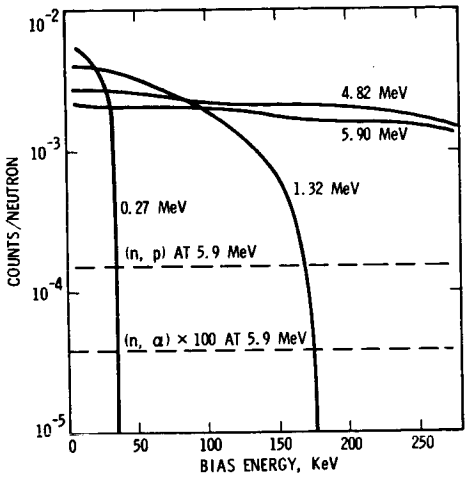

FIGURE 4. Neutron Response of A 300μ Silicon Detector

Since the energy tranferred to the silicon by neutrons is 0.133 En $\sin^2(\theta_{c.m.}/2)$, the maximum energy of the silicon recoil $\hat{E}_{si}$, is obtained when $\theta_{c.m.} = 180^\circ$ and the energy distribution function for the silicon nuclei after collision is $1/\hat{E}_{si}$. The probability function is given by $1 - (E_B/\hat{E}_{si})$ and the response function is

$$R(E_n, E_B) = \epsilon_D(E_n, t)\left[1 - \frac{E_B}{.133 E_{si}}\right] \quad (4)$$

In Figure 4, this function is plotted for various neutron energies and for various bias energies. The contribution from protons generated in (n,p) reactions and the contribution from α particles generated in (n,α) reactions are indeed small. At low neutron energies these charged particles do not exist and at high energies, the contribution from protons is more than an order of magnitude lower and the contribution from α particles is about 5 orders of magnitude smaller than the pulse height generated by elastic scattering of neutrons. Therefore, up to 5 MeV the major portion (~99%) of counts comes from the silicon nuclei after being struck by neutrons and at 6 MeV nearly 90% of the response is due to this reaction. The protons and particles generated within the detector are completely absorbed since the edge effects are small. Because of this they must be included in the pulse height calculation since the time interval for the ionization process is much smaller than the charge collection time interval and the deposited energy is equal to the maximum energy if it is above the bias energy.

The neutron flux from the fuel capsule can also be folded into the response function, thus, in the $(o, \hat{E}_n)$ energy interval the response of the silicon detector at E_n is

$$dR(E_n)/dE_n = \phi(E_n) A \epsilon_D(E_n) P(E, E_B) / \phi_o \quad (5)$$

A is the detector's cross-sectional area and $dR(E_n)/dE_n$ is given in $c/(n/cm^2)$/MeV. The total silicon response for a polyenergetic neutron beam with energies up to $\hat{E}_n$ is

$$R(\hat{E}_n) = \int_{(E_n)_{min}}^{\hat{E}_n} A \phi(E_n) \epsilon_D(E_n) P(E, E_n) dE_n \quad (6)$$

$(En)_{min}$ is the minimum neutron energy allowed for a given bias energy, i.e., 7.55 E_B.

Equation 4 is plotted in Figure 5 for the same neutron energies utilized in Figure 4. $R(E_n)$ is given in counts/sec for neutron energies from (E_n) min up to $\hat{E}_n$. The total counting rate at a a given maximum neutron energy depends on the bias energy. At 100 keV bias energy and at 5 MeV neutron energy the counting rate is about 20 c/sec.

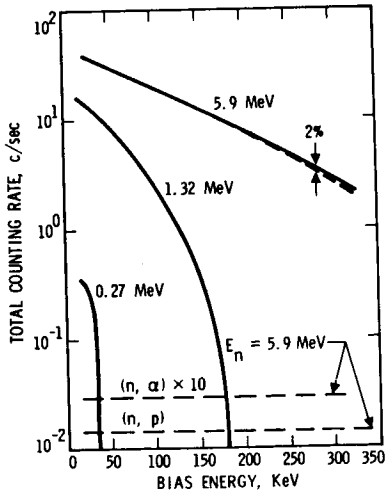

FIGURE 5. Total Counting Rate of A 300μ Silicon Detector

PULSE HEIGHT DEFECTS

The response functions which were calculated in the previous section are yet subject to another restriction namely the pulse height defect (PHD). This effect is more pronounced in the case of silicon detectors because the pulse height (PH) is mainly due to the elastic scattering of neutrons.

Neutrons transfer their energies to the silicon sensitive medium by atomic scattering and nuclear ractions rather than through an electronic ionization process. The secondary charged particles produced by the neutron interaction such as protons, alpha particles and silicon nuclei in turn transfer their energies to the medium via ionication and nuclear charge scattering. The photons generated in the (n,Y) and (n,n'Y) reactions escape the medium in most cases, thus will not deposit energy. The ionization processes contribute to the PHD. Ionization causes the displacement of electrons while nuclear charge scattering (Rutherford scattering) causes the displacement of atoms from their equilibrium position and leaves vacancies in the lattice. In Table 1, the maximum energies and ranges of the protons, alpha particles and silicon nuclei are presented. Since we have selected 300μ for the depletion depth of the detector, nearly all these charged particles remain inside. The energy transferred to the silicon is $\hat{E}_{Si} \sin^2(\theta_{cm}/2)$ where $\hat{E}_{Si}$ is the maximum transmitted energy. If r is the ratio of the mass of the silicon atom over the mass of the ith charged particle, namely (α,p,S_i) then

$$\hat{E}_{Si} = 4 r_i E_i (1+r_i)^{-2}$$

Since $r_{Si} = 1$, $r_p = 28$ and $r_\alpha = 7$, the maximum energies are $\hat{E}_{Si} = E_{Si}$, $\hat{E}_{Si} = .1332\ E_p$ and $\hat{E}_{Si} = 0.4328\ E_\alpha$. If we use the maximum energies of the charged particles for a 6 MeV neutron beam from Table 1, then the maximum transmitted energies are 798, 240 and 1170 keV for S_i,p and α particles, respectively. However, in the real case only a fraction of these energies are transmitted to the medium via non-ionizing processes, the remainder contribute to the PH.

Figure 6 presents the fraction of the PHD as a function of the charged particle energy and considers up to two neutron scatters.[4] We notice that the PHD is important only at low energies and within this range the PHD due to the silicon nuclei is much greater than the PHD due to protons or α alpha particles. For example, for a 100 keV charged particle (4.5, 4.0 and 0.75 MeV neutron energies for proton, particle and S_i, respectively) the PHD due to S_i is about 60 keV while for protons it is 6 keV and for α particles it is 12 keV.

We now can include the pulse height defects into the silicon responses presented in Figure 4.

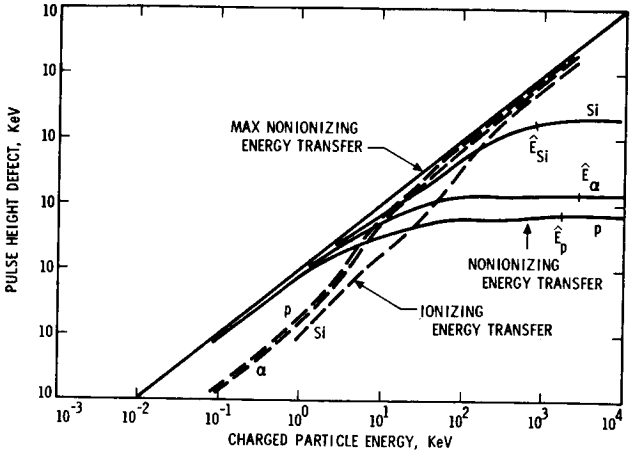

FIGURE 6. Pulse Height Defect for Silicon

For 1.32 MeV neutrons, we are concerned only with silicon nuclei which have a maximum energy of 175 keV, thus if the bias energy is set at higher values there would be no response. The PHD at this energy indicates (Figure 6) that 58% of energy is transmitted to the medium by the nonionizing processes, thus the bias energy needs to be set even lower (74 keV) if any response is desired. At high neutron energy (i.e., 6 MeV) the maximum energy of the charged particles is given in Table 1, and the PHD's are 48, 159 and 528 keV for protons, alpha particles and silicon nuclei respectively. This means protons and particles will contribute to the total response but there will be no pulse height due to the (n,n) reaction if the bias energy is greater than 270 keV.

RESPONSE OF A SHIELDED DETECTOR

Monte Carlo calculations were performed to estimate the response of a shielded 300 micron thick silicon detector to incident monoenergetic neutrons of 0.201, 1.49, and 5.18 MeV. The detector response mechanism analyzed was based on secondary gamma radiation from neutron capture (n,Y) and inelastic scattering (n,n',Y) reactions taking place both in the silicon and the 86 mil aluminum shield over the front end of the detector upon which neutrons were assumed to be normally incident.

Since the neutron interaction probabilities were small for the combined detector assembly i.e., approximately 0.03, 0.044, and 0.066 for the 5.18, 1.49, and 0.201 MeV neutrons, respectively; secondary photon sources for the shielding and detector volumes were determined assuming exponential attenuation of the incident parallel beam neutrons in the detector materials. The secondary gamma sources from the (n,γ) and (n,n',γ) reactions were assumed to be isotropic. Monte Carlo calculations were then performed to simulate the photon transport and electron transport in the detector materials and energy deposition in the 300 micron, 2.0 cm^2 silicon detector. The secondary source terms were determined using the POPOP-4 Program and source library (2)

GEOMETRY

The model which was used in the analysis is given by the configuration shown in Figure 7. As shown it is composed of three cylindrically symmetric material regions; these are the 0.03 cm x 2.0 cm^2 silicon, the aluminum holder, and the 86 mil aluminum shield. Secondary gamma ray sources were specified for the shaded portion (designated, S_1) of the aluminum shield coincident with a radial neutron beam dimension of 1.38 cm; this corresponds to the intersection at the front surface of the Al shield made by the projection of the detector holder front bevil. The calculations were performed such that secondary gamma ray sources originating in S_1, assumed to be isotropic, were biased toward the silicon detector volume, itself a secondary gamma ray source volume designated as S_2. In view of the fact that a large proportion of the secondary photon spectrum is high enough in energy to give rise to electrons (from primarily Compton interactions) whose ranges exceed the aluminum shield thickness, a biasing region on the silicon side of the aluminum shield was not specified. As the secondary sources were based on those portions of the configuration designated S_1 and S_2 in Figure 7, secondary photons originating in the holder and other portions of the aluminum shield were neglected The secondary gamma ray sources originating in the holder may not necessarily be insignificant, however, this particular analysis has been restricted to only analyzing the detector response relating to the effect of the front 86 mil aluminum shield.

SECONDARY GAMMA RAY SOURCE

This analysis considers secondary gamma ray sources which originate in the 86 mil aluminum shield and the 300 micron thick silicon detector from neutron capture (n,γ) and inelastic neutron scattering (n,n',γ). The secondary gamma ray source term is given as

$$S_r(\vec{r}, E_n, E_g) = \phi(\vec{r}, E_n) N(\vec{r}) \sigma(E_n) Y(E_n, E_g)$$

where, r = position vector, E_n = neutron energy, Eg = gamma energy, $\phi(E,E_n)$ = neutron flux, n/cm^2-sec, N(r) = atom density, atoms/cm3, $\sigma(E_n)$ = reaction cross section for gamma production, cm^2/atom and, $Y(E_n,Eg)$ = gamma yield, photons/neutron reaction.

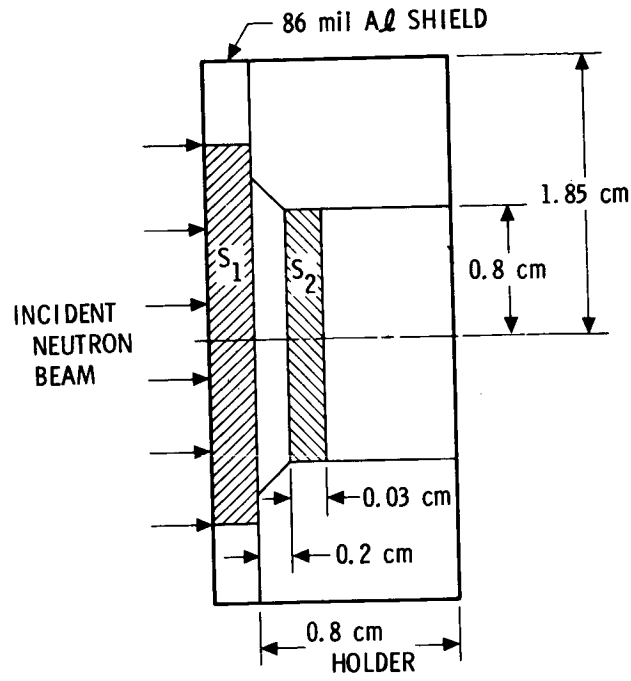

FIGURE 7. Silicon - Aluminum Configuration

The reaction product, $\sigma(E_n)\ Y(E_n,Eg)$, was computed using the POPOP-4 Program and library data. The reaction cross sections, i.e., $\sigma^{n,\gamma}(En)$ and $\sigma^{nn'\gamma}(En)$ for the (n,γ) and (n,n',γ) reactions, respectively, were taken from reference (3) with the exception of $\sigma^{n,n',\gamma}$ for silicon, which was included in the POPOP-4 library data.

The (n,γ) reaction yields are based on thermal neutron reactions and are thus assumed constant over neutron energy, i.e., $Y_{n,\gamma} = Y(Eg)$ and the inelastic neutron scattering gamma rays are a function of both neutron energy and gamma energy, i.e., $Y_{n,n'\gamma} = Y(Eg,E\gamma)$.

Calculations were performed using the RAMPARTS(1) Monte Carlo program by random sampling of the secondary gamma ray source term $S_r(\vec{r}, E_n, E_g)$ over S_1 and S_2 (Figure 7) with equal weighting. Spatial sampling of $S_r(\vec{r}, E_n, E_g)$ in the cylindrical source geometry was based on assuming a constant distribution radially and azimuthally. The distribution in Z was assumed exponential, $\phi_0 \exp(-N\sigma_T z)$ for which $N\sigma_T(E_n) z << 1$, becomes essentially linear, $\phi_0(1 - N\sigma_T z)$

Individual photon energies were selected by random sampling of the gamma ray energy spectra. Photon transport within the configuration given in Figure 7 was allowed to proceed allowing up to two collision points. Biasing of the photon transport was imposed in order to reduce the calculational varience such that the silicon was preferred with a weight of 100:1 and the aluminum shield 10:1. Consequently, the detector holder was accordingly deemphasized in this study. Further biasing of 10:1 was imposed on picking the radial dimension of the cylindrical source coordinate, and the initial direction of the photons, in order to minimize the calculational varience from the standpoint of obtaining a reasonable amount of samples in S_2 in view of the primary electron range consideration.

Primary electron sources from pair production and Compton scattering reactions of the gamma rays were simulated from which points electron transport was simulated using a Moliere type angular straggling model together with energy loss and angular deflection evaluated at 4% energy loss intervals, and allowing a maximum of up to 50 collisions for the electrons.

The secondary gamma ray sources are normalized to the total number of photons, in each of source volumes S_1 of S_2.

Results of these initial response calculations of a 300 micron silicon detector to incident neutrons are plotted in Figure 8. In general, these calculations suggest that response to neutrons, due to the generation of secondary gamma rays, are about 3 to 4 orders of magnitude below incident photons on a one-for-one basis. The channel energy bias counts per incident neutron normalized over a 2.01 cm^2 area (area of the 300μ detector) are given along with calculational error for the 3 neutron energies shown. The response values are also broken up into contributions from both neutron capture gamma (n,γ) and inelastic neutron scattering gamma $(n,n'\gamma)$ reactions occuring collectively in the aluminum 86 mil shield and 300 micron silicon detector. (For 0.201 MeV neutrons, no values are given for $(n,n'\gamma)$ reactions since this is below the threshold level for the first excited state).

The relative contribution to the response of electrons born in the aluminum shield and the silicon-born electrons to aluminum-born electrons. For the 5.18 MeV incident neutrons, silicon-born electrons are more important than aluminum shield-born electrons for the $n,n'\gamma$ reactions, i.e., 6.2:1. This can be related to the relatively large spectral gamma component at 1.5 to 2.0 MeV. The situation for 1.49 MeV neutrons is somewhat reversed, although the reversal is not as dominate. An inspection of the input spectra used suggest competition between n,γ reaction electrons in silicon and (n,n',γ) reaction electrons from the aluminum shield, with the latter being lower energies. These lower energy electrons would have smaller ranges which allow perhaps only a small proportion of them to escape from the aluminum shield and enter the silicon to add to the response, and thus disallow any possible spectral advantage as compared to the (n,γ) reactions in silicon. What is somewhat surprising for this case is why the (n,n',γ) gamma reactions are not more important in view of the essentially large single line secondary gamma component in silicon at 1.0 to 1.5 MeV.

Figure 4 gives a plot of the results for the three neutron energy cases for which these calculations were performed. The relatively large response shown for the 0.201 MeV neutron case is due primarily to the increase in the n,γ cross section, coupled with the assumed thermal neutron reaction secondary gamma yields. In fact, under these assumptions, these would be a continuing upward trend with decreasing neutron energy.

*G. Anno; ART Corporation, L. A., California

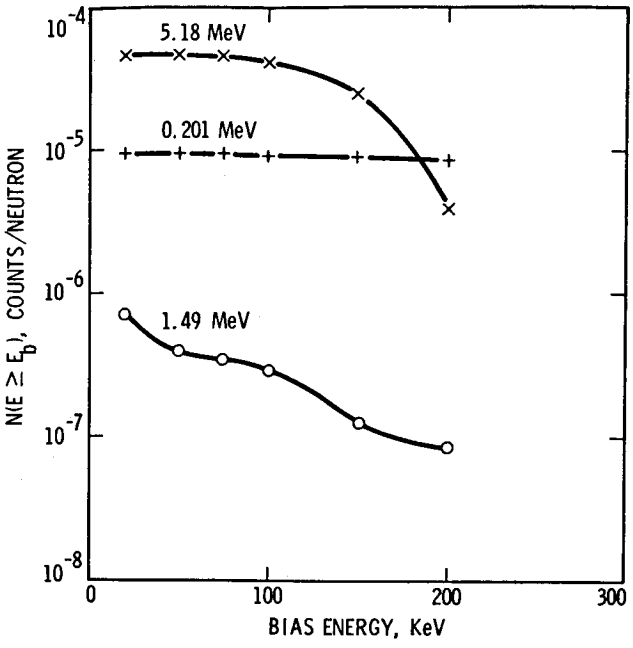

FIGURE 8

CONCLUSIONS

The following general conclusions can be made from the results.

1. In the neutron energy range of .27 to 6 MeV and 25 to 250 keV bias energy the maximum response of a 300μ silicon detector is about 4 x 10^{-3}c/n.

2. At 3 MeV neutron (or gamma ray) energy and 50 keV electron bias energy the response of the silicon detector to neutrons is about 11% of the response to the source gamma rays. (i.e., R_n = .0029 and R_γ = .025 M. Reier, JPL, 1970).

3. The contribution from the secondary particles generated in the shield is about 3 to 4 orders of magnitude smaller than the response to the source neutrons.

4. At 50 to 250 keV bias energy range and for a neutron flux emitted from a 2 KW MHW PuO_2 fuel power source the counting rate is estimated at about 31 to 5 counts/sec.

ACKNOWLEDGEMENT

The authors wish to express their appreciation to Dr. Melvin Reier of JPL for his valuable discussion during this investigation.

REFERENCES

1. T. M. Jordan, "Beta- A Monte Carlo Computer Program for Bremsstrahlung and Electron Transport Analysis," AFWL-TR-68-111, October, 1968.

2. W. E. Ford III and D. H. Wallace, "A Code for Converting Gamma Ray Spectra to Secondary Gamma Production Cross Sections" CTC-12. (May 23, 1969).

3. J. W. Ray et. al., "Neutron Cross Sections of Nitrogen, Oxygen, Aluminum, Silicon, Iron, Deuterium, and Bergllium," UNC-5139, (Nov. 1965).